Received: 10 May 2020 | Revised: 7 January 2021 | Accepted: 8 January 2021

DOI: 10.1096/fj.202001160RR

RESEARCH ARTICLE

THE FASEB JOURNAL

GSE4-loaded nanoparticles a potential therapy for lung fibrosis that enhances pneumocyte growth, reduces apoptosis and DNA damage

Laura Pintado-Berninches[1,2] | Ana Montes-Worboys[3] | Cristina Manguan-García[1,2] | Elena G. Arias-Salgado[1] | Adela Serrano[4,5] | Beatriz Fernandez-Varas[1] | Rosa Guerrero-López[1,2] | Laura Iarriccio[1] | Lurdes Planas[3] | Guillermo Guenechea[2,6] | Susana P. Egusquiaguirre[7] | Rosa M. Hernandez[7] | Manoli Igartua[7] | Jose Luis Pedraz[7] | Julio Cortijo[4,5] | Leandro Sastre[1,2] | Maria Molina-Molina[3,5] | Rosario Perona[1,2]

[1]Instituto de Investigaciones Biomédicas, CSIC/UAM, IDIPaz, Madrid, Spain

[2]Centro de Investigación Biomédica en Red de Enfermedades Raras (CIBERER), Madrid, Spain

[3]ILD Unit, Pneumology Department, University Hospital of Bellvitge, IDIBELL, University of Barcelona, Hospitalet de Llobregat, Barcelona, Spain

[4]Department of Pharmacology, Faculty of Medicine, University of Valencia, Valencia, Spain

[5]CIBER of Respiratory diseases (CIBERES), Health Institute Carlos III, Madrid, Spain

[6]Division of Hematopoietic Innovative Therapies, Centro de Investigaciones Energéticas Medioambientales y Tecnológicas (CIEMAT), Instituto de Investigación Sanitaria Fundación Jiménez Díaz (IIS-FJD/UAM), Madrid, Spain

[7]NanoBioCel Group, Laboratory of Pharmaceutics, School of Pharmacy, University of the Basque Country (UPV/EHU), CIBER-BBN, Vitoria-Gasteiz, Spain

Correspondence
Rosario Perona, Instituto de Investigaciones Biomédicas, CSIC/UAM, C/Arturo Duperier, 4, Madrid 28029, Spain.
Email: rperona@iib.uam.es

Funding information
CIBER, Grant/Award Number: 576/805_ER16PE06P2016; MINECO, INNPACTO, Grant/Award Number: IPT-2012-0674-090000; Fondo de Investigación Sanitaria. Instituto de Salud Carlos III (FEDER funds), Grant/Award Number: PI18/00367 and P17-01401; CICYT,

Abstract

Idiopathic pulmonary fibrosis is a lethal lung fibrotic disease, associated with aging with a mean survival of 2-5 years and no curative treatment. The GSE4 peptide is able to rescue cells from senescence, DNA and oxidative damage, inflammation, and induces telomerase activity. Here, we investigated the protective effect of GSE4 expression in vitro in rat alveolar epithelial cells (AECs), and in vivo in a bleomycin model of lung fibrosis. Bleomycin-injured rat AECs, expressing GSE4 or treated with GSE4-PLGA/PEI nanoparticles showed an increase of telomerase activity, decreased DNA damage, and decreased expression of IL6 and cleaved-caspase 3. In addition, these cells showed an inhibition in expression of fibrotic markers induced by TGF-β

Abbreviations: AECs, alveolar epithelial cells; AECII, alveolar type II cells; CTGF, connective tissue growth factor; CXC12, chemokine ligand 12; ECM, extracellular matrix; FPF, familiar pulmonary fibrosis; GSE, Genetic suppressor element; IL6, Interleukin 6; IL-11, Interleukin 11; IPF, Idiopathic pulmonary fibrosis; Micro-SPECT-CT, micro-Single Photon Emission Tomography/Computed tomography; PDGF, platelet-derived growth factor; proSP-C cells, pro-surfactant protein expressing cells; TGF-β, Tumor growth factor β; TIFs, telomere-associated foci; TNFα, tumor necrosis factor alpha; α-SMA, α-smooth muscle actin protein.

Laura Pintado-Berninches, Ana Montes-Worboys, and Cristina Manguan-García contributed equally to the experimental work.

Leandro Sastre, Maria Molina-Molina, and Rosario Perona contributed equally as corresponding authors.

Grant/Award Number: SAF2014-55322-P; MINECO/FEDER funds, Grant/Award Number: SAF2015-68073-R

such as collagen-I and III among others. Furthermore, treatment with GSE4-PLGA/PEI nanoparticles in a rat model of bleomycin-induced fibrosis, increased telomerase activity and decreased DNA damage in proSP-C cells. Both in preventive and therapeutic protocols GSE4-PLGA/PEI nanoparticles prevented and attenuated lung damage monitored by SPECT-CT and inhibited collagen deposition. Lungs of rats treated with bleomycin and GSE4-PLGA/PEI nanoparticles showed reduced expression of α-SMA and pro-inflammatory cytokines, increased number of pro-SPC-multicellular structures and increased DNA synthesis in proSP-C cells, indicating therapeutic efficacy of GSE4-nanoparticles in experimental lung fibrosis and a possible curative treatment for lung fibrotic patients.

KEYWORDS

alveolar cells, GSE4, pulmonary fibrosis, telomerase

1 | INTRODUCTION

Idiopathic pulmonary fibrosis (IPF) is an age-associated chronic, progressive, and lethal lung disorder of unknown etiology with few therapeutic options that modify its natural history.[1] The disease occurs in middle aged and elderly adults, although the familial forms (FPF) may present in younger individuals. Lung fibrosis is an aberrant wound healing response after alveolar injury characterized by the presence of lung scarring with immune and mesenchymal abnormalities, in which the restitution of epithelial integrity and tissue function are compromised. The mechanisms responsible for the defective repair and regeneration are poorly understood. However, recent studies suggest a possible role of accelerated aging and telomere attrition in the onset of the disease mainly associated to the familiar forms.[2] Therapies based on anti-inflammatory agents have little impact on disease progression,[3] although recent findings on the role of IL-11 are promising.[4] Anti-fibrotic therapy based on the small molecules nintedanib[5] and pirfenidone[6] have been approved for the treatment of IPF, but both drugs show important toxicities. Furthermore, although new drugs have been used in clinical trials,[7] no relevant results have been reported, therefore, new approaches are needed to advance in the treatment of IPF.

Telomere shortening contributes to physiological aging and to age-related diseases.[8,9] Animal models have shown that with increased age or telomere attrition, the lungs become highly susceptible to injury and can develop progressive fibrosis without the need for repetitive injury.[10,11] Mutations in telomerase and shelterin genes cause accelerated telomere shortening and several telomere syndromes. Mutations in *TERT, TERC, TINF2, RTEL, PARN, NAF1, ACD, NOP10, NHP2,* and *DKC1* have been identified in pulmonary fibrosis.[12-16] Interestingly, telomere shortening has been found in 25% of IPF and 50% of FPF patients.[17] The mechanism by which telomere shortening induces lung fibrosis is not well understood but some reports suggest an increase of cell senescence (in both fibroblasts and alveolar cells), induction of profibrotic pathways such as transforming growth factor (TGF-β/Smads signaling)[18] and alveolar stem cell failure.[19] Intratracheal administration of bleomycin in rats or mice has been widely used to study lung injury and fibrosis and to evaluate anti-fibrotic therapies. Mice with telomere shortening die when challenged with bleomycin, indicating an essential role of telomerase in alveolar cell repair[19] and in senescence prevention.[20]

The transforming growth factor beta (TGF-β) pathway, among others, is considered as a central driver of pathogenesis of IPF.[18] Activated fibroblasts or myofibroblasts have been described as the source of extracellular matrix (ECM) deposition during fibrogenesis. However, evidence from animal models and in vitro studies has suggested an implication of alveolar type II cells (AECII) by induction of epithelial mesenchymal transition.[21-23] In IPF lungs, activated AECII express several cytokines such as platelet-derived growth factor (PDGF), TGF-β1, tumor necrosis factor (TNF), endothelin-1, connective tissue growth factor (CTGF), osteopontin, and CXC chemokine ligand 12 (CXCL12), and promote profibrotic responses.[7,24,25] Human AECII are able to undergo, in vitro, a phenotypic change upon TGF-β-stimulation and acquire the capability to produce collagen as well as display phenotypic changes on gene expression that resemble Type 2 EMT. Therefore, in addition to activated fibroblasts, these cells might contribute to the pool of collagen-secreting cells in the alveolar compartment during wound healing processes or fibrotic reactions.[26]

We have previously described that a 55 amino acids-long fragment of the dyskerin TruB domain, named GSE24.2,

and a shorter derived peptide, GSE4, have protective effects on dyskeratosis congenita (DC) and ataxia telangiectasia (AT) patient cells.[27-30] GSE4 peptide increased telomerase activity and reduced DNA damage, oxidative stress, cell senescence, and increased DNA synthesis in DC and AT patient cells.[29] GSE4 expression also activated TERT promoter and increased TERT and TERC gene expression.[29] Taking into account the effect that GSE4 has on DNA damage in different disease model cell systems,[27-30] and the role of DNA damage and oxidative damage in lung injury during fibrosis pathology, we explored the possible therapeutic effect of GSE4 in IPF. Using PLGA/PEI nanoparticles as a drug delivery system, we aimed to explore the effects of GSE4 expression or GSE4-PLGA nanoparticles treatment in alveolar epithelial cells and in a rat model of lung fibrosis.[30-32] Our results demonstrated that expression of GSE4 increased telomerase activity, decreased DNA damage, inflammatory cytokine levels and apoptosis in rat type II alveolar cells. Moreover, in rats treated with bleomycin, GSE4-PLGA/PEI nanoparticles prevented and reduced pulmonary fibrosis as detected by imaging and histological techniques. Our results suggest that GSE4 should be considered as a new potential treatment for patients with pulmonary fibrosis.

2 | MATERIALS AND METHODS

2.1 | Cell lines

RLE-6TN (ATCC CRL-2300) cell line was purchased from ATCC (Manassas VA, USA). Cells were cultured in HAM´s F12 (Gibco, Life Technologies, Thermo Fisher Scientific, Waltham, MA, USA) and supplemented with fetal bovine serum (FBS) (Gibco), penicillin (100 U/mL)/streptomycin (100 µg/mL) solution (Gibco), 2 mM L-glutamine (Gibco), 0.01 mg/mL bovine pituitary extract (Gibco), 0.005 mg/mL insulin (Gibco), 2.5 ng/mL insulin-like growth factor (Gibco), 0.00125 mg/mL transferrin (Gibco), and 2.5 ng/mL EGF (Gibco) and maintained at 37°C in a humidified 5% CO2 atmosphere.

2.2 | Western blot analysis

2.2.1 | Antibodies

The source of antibodies was as follows: phospho-Histone H2A.X Ser139 (2577; Cell Signaling Technology, Danvers, MA, USA), phospho-p38 and p38 (Th180/tyr182 (9211; Cell Signaling), caspase 3 (9662; Cell Signaling) α-tubulin (T9026; Sigma-Aldrich Inc Missouri, USA), and anti-Phospho-p53 (ser15, 9284; Cell Signaling).

2.2.2 | Western blot

Whole cell extracts from RLE-6TN were prepared using lysis buffer (25 mM HEPES pH 7.5, 0.3 mM NaCl, 1.5 mM $MgCl_2$, 0.2 mM EDTA, 20 mM β-glycerophosphate, and 0.1% Triton X-100) and a protease inhibitor cocktail (0.5 mM ABSF, 2 µg/mL Leupeptin, 2 µg/mL aprotinin, 0.5 mM DTT, and 0.1 mM Na_3VO_4). Lysates were centrifuged and protein concentration was measured by using the Bio-Rad protein assay (500-0006; Bio-Rad Hercules, CA, USA). A 20 µg of protein extracts were resolved on SDS-polyacrylamide and electroblotted to Immobilon P membranes (Millipore, Thermo Fisher Scientific, Waltham, MA, USA). Western blot analysis was conducted by using ECL reagent (Santa Cruz Biotechnology, Dallas, TX, USA).

2.3 | Immunofluorescence and Telomere-Induced Foci evaluation

Protein localization was carried out by fluorescence microscopy. For this purpose, cells were grown on coverslips, transfected and fixed in 3.7% of formaldehyde solution (47 608; Fluka, Sigma-Aldrich Inc Missouri, USA) at room temperature for 15 minutes. After washing with 1x PBS, cells were permeabilized with 0.2% of Triton X-100 in PBS and blocked with 10% of horse serum before overnight incubation with anti-γ-H2A.X antibody, (05-636; Merck Millipore, Thermo Fisher Scientific, Waltham, MA, USA). Finally, cells were washed and incubated with secondary antibodies coupled to fluorescent dyes (Alexa Fluor 488 or/and Alexa Fluor 647). At least 200 cells were quantified in each experimental condition.

For Telomere-induced foci (TIF) evaluation cells were co-immuno stained with anti-TRF1 and anti-γ-H2A.X antibodies. Imaging was carried out at room temperature in Vectashield, mounting medium for fluorescence (Vector Laboratories, Burlingame, USA). Images were acquired with a Confocal Spectral Leica TCS SP5. Microscope using an HCX PL APO Lambda blue 6361.40 OIL UV, zoom 2.3 lens using LAS-AF 1.8.1 Leica software and processed using LAS-AF 1.8.1 Leica software and Adobe Photoshop CS. Co-localization of TRF1 and γ-H2A.X was quantified in at least 200 cells in each condition.

2.4 | Rat model of bleomycin-induced lung fibrosis

Animal studies were made in accordance with European Community Directive and Spanish guidelines for the use of experimental animals and approved by the

institutional committee of animal care and research. To check if GSE4-nanoparticles were able to reach the lungs and rescue telomerase activity in rats, we used Wistar rats (Wistar Han, 9 weeks old and weighing 250-350 g) that were inoculated intraperitoneal once with GSE4-nanoparticles (equivalent of 15 μg peptide/200 gr rat) and 24 hours later intratracheal instilled with a single dose of bleomycin (Bleo) (3.75 U/kg) to induce lung injury.[33-35] Three days later lungs were isolated, one lung was used for protein extraction for TRAP assays and the other for immunohistochemistry analysis. Twenty-four rats were used for each experiment and were divided into four groups: control-PBS (n = 4), control-GSE4 (n = 4), Bleo-PBS (n = 8), and Bleo-GSE4 (n = 8). The study was repeated three times.

For pharmacological studies, we used the same rat model that facilitated imaging studies and tissue availability and two different pharmacological models. In the preventive model, Wistar rats were intratracheal instilled with a single dose of bleomycin (Bleo) (3.75 U/kg) to induce lung injury, GSE4-nanoparticles (equivalent of 15 μg peptide/200 gr rat) or vehicle (filtered Phosphate-Buffered Saline-PBS) were administered intraperitoneal from day −1 and every 96 hours for 14 days. The therapeutic protocol was exactly the same but starting GSE4-nanoparticles administration on day 5 after Bleo instillation, and then, repeated every 96 hours for 9 days. Twenty-six rats were used for each experiment and divided in four groups: control-PBS (n = 4), control-GSE4 (n = 4), Bleo-PBS (n = 8), Bleo-GSE4 (n = 8), and two rats were only observed as sham. Each experimental study was repeated three times.

Animals were weighed periodically throughout the procedure and their evolution was controlled using a multimodal imaging system micro-Single Photon Emission Tomography (SPECT)/Computed Tomography (CT)). At the end of the treatment period, rats were euthanized and lungs were extracted. Rats were used according to protocols approved by Comunidad de Madrid and CSIC animal care and use Committee.

2.5 | Telomeric repeat amplification protocol (TRAP) assay

Telomerase activity was determined under recommended standard conditions of the TRAPEZE Telomerase Detection S7700 Kit (Millipore, Thermo Fisher Scientific) for telomeric repeat amplification (TRAP) using radioisotopic detection. Telomerase activity was determined in each sample using 0.5, 0.25, and 0.125 μg of protein extract and normalized with the internal control included in the assay.[27]

2.6 | Real-time quantitative PCR

Total RNA from RLE-6TN cells and animal tissues was obtained using the TRIzol reagent (Invitrogen, Thermo Fisher Scientific, Waltham, MA, USA). RNA was converted to cDNA using random primers and the High-Capacity cDNA Archive Kit (Applied Biosystems, Thermo Fisher, Scientific Waltham, MA, USA). Quantitative PCR was made using the Power SYBR kit and the StepOne Plus Real-Time PCR System (both from Applied Biosystems). Relative expression levels were calculated using the comparative threshold cycle method[36] and GAPDH as internal control. Oligonucleotides used are listed in Table 1. Rat IL6 and CDKN1A expression study was performed by using the TaqMan probes Rn01410330_m1 and Rn01427989_s1, respectively.

TABLE 1 Primer sequence, 5′–3′

Gene name	Forward	Reverse
TENASCIN-C	ATGTTGAATGGCGACAC	CGGTCTCCAAACCCAG
COLLAGEN I	TGCTTGAAGACCTATGTGGGTA	AAAGGCAGCATTTGGGGTAT
TGF-β1	AGAACCCCCATTGCTGTCCC	GAAAGCCCTGTATTCCGTCTCC
FGF-2	GAACCGGTACCTGGCTATGA	CCGTTTTGGATCCGAGTTTA
TGF-βR-1	AGAAAGCATCGGCAAAGGTC	CCCAGGATATTTTCATGGCG
MCP-1	CACCTGCTGCTACTCATTCACTG	CTTCTTTGGGACACCTGCTGCT
PAI-1	TGAGATCAGTACTGCGGACG	GAGGGGCACATCTTTTTCAA
α-SMA	AAGAGGAAGACAGCACAGCTC	GATGGATGGGAAAACAGCC
VIMENTIN	TGACCGCTTCGCCAACTA	CGCAACTCCCTCATCTCCT
GADPH	ACCACAGTCCATGCCATCAC	TCCACCACCCTGTTGCTGTA
COLLAGEN III	GATGGCTGCACTAAACACACT	CACTTTCACTGGTTGACGAGA
TERT	GAGTGTCACTAAGGGCCAAG	CAGCTGCAGTCTTAAGGAGG
TERC	CGTGAAGAGCTAGTCTCTG	GGTTGTAGGAACTGAGTTCC
GSE4	GATGGGTTTCATTAATCTTGACAAGCCCTCTAACCCCTAAG	GGAATGCTCGTCAAGAAGAC
SCRAMBLE	GATGCTTTCTAAGGGTAATAACATTCCCGACTTCCCCTAAG	GGAATGCTCGTCAAGAAGAC

2.7 | Lentiviral vector production and cell transduction

Lentiviral vector expressing GSE4 from the pRRL-CMV-IRES-EGFP vector were described in Ref. ([29,30]). Lentiviral vectors were produced using HEK 293T cells transfecting the pRRL-CMV-IRES-EGFP (empty or scramble vector) and expressing GSE4 (pRRL-CMV-GSE4-IRES-EGFP) together with pCD-NL-BH and pMD.2G VSV.G packaging plasmids. Seventy-two hours after transfection, supernatants were recovered and used to transduce cell lines in the presence of polybrene (5 μg/mL). Cell lines were characterized by measuring expression of GSE4 RNA. Efficiency of expression was measured by evaluating EGFP expression by flow cytometry. Experiments were carried out when the percentage of cells expressing GFP was higher than 85%.

2.8 | Nanoparticle synthesis and loading of scramble and GSE4 peptides

Chemically synthesized scramble and GSE4 peptide labeled with FITC were obtained from ChinaPeptides Co., Ltd. (Hangzhou, China) and purified by HPLC. PLGA/PEI nanoparticle preparation and scramble and GSE4 loading were performed as previously described.[31,32] Internalization efficiency was estimated by determination of intracellular fluorescence using a fluorescence ELISA reader.

2.9 | Micro-SPECT-CT

For SPECT/CT acquisition images, on days 0, 7, and 14; 500 μCi of ^{99m}Tc-MAA (macroaggregated serum albumin, MAA) were injected in the tail vein. Thirty minutes after the administration; animals were anesthetized and introduced in multimodal acquisition equipment (Albira; Oncovision Gem-Imaging SA, Valencia, Spain). Previously, SPECT studies were programed with a field of view (FOV) of 80 mm, capture time 30 minutes, 60 projections per second, and a Pinhole collimator. And X-rays for CT acquisition were programed with 400 uA intensity current, voltage 45 kV, and a filter attenuation of 0.5 mm; such intensity equivalent to an equivalent dose of 220 mSv and effective dose of 357.4 mSv. These doses are 20 times lower than reported LD_{50} dose[37] 30 minutes after the administration; animals were anesthetized and introduced in multimodal acquisition equipment (Albira; Oncovision Gem-Imaging).

The images were reconstructed using the algorithm FBP (Filtered Back Projection) using the Standard parameters reconstruction Albira Suite 5.0 Reconstructor. The combination of acquisition and reconstruction result in a final image matrix 255 × 255 × 255 pixel size of 0.25 × 0.25 × 0.25 mm. The images were analyzed and quantified by Analysis software PMOD 3.2 (PMOD Technologies LTD, Zurich, Switzerland).

2.10 | Immunohistochemistry analysis

Formalin-fixed, paraffin-embedded lung tissue sections (5 μm) were de-waxed with Xylene and rehydrated through a series of alcohols to water. Antigen retrieval was performed using an unmasking buffer pH 9 (10 mM Tris Base, 1 mM EDTA Solution, 0.05% Tween 20) in a microwave oven for 20 minutes. Sections were blocked with a Goat Serum blocking solution (5% Goat serum, 1% BSA, 0.2% Triton-X-100 in PBS pH 7.1) for 45 minutes, and then, incubated with primary antibodies at 4°C overnight in a humidity chamber. Primary antibodies used were: Dilution 1:2000 rabbit anti-Pro-surfactant Protein-C, proSP-C (cat#AB3786 Millipore, Thermo Fisher Scientific, Waltham, MA, USA); Dilution 1:100 mouse monoclonal anti-Ki67 (cat# 550609 Becton Dickinson, Franklin Lakes, New Jersey, USA); Dilution 1:100 anti-Phospho-Histone H2A.X (Ser139), clone JBW301 (Cat# 05-636 Millipore), anti-alfaSMA, clone 1A4 (cat# A5228 SIGMA) anti-TNFα (cat# SC52746 Santa Cruz Biotechnology, Dallas, Texas, USA). Sections were washed with PBS with 0.2%Triton-X-100 and incubated with the secondary antibodies for 45 minutes at room temperature. DAPI (D1306 Molecular Probes, Thermo Fisher, Scientific Waltham, MA, USA) or ToPro-3 (T3605 Molecular Probes) was used for DNA nuclear staining and slides were then mounted using ProLong Diamond antifade reagent (P36970 Molecular Probes). All images were acquired using a LSM710 (Zeiss) confocal microscope. All objectives were plan-apochromatic. Sequential scanning mode was used to avoid crosstalk between channels. All images correspond to a maximal projection and were processed with Zen2009 and Image J software for quantification. Quantification was performed determining the number of cells positive for a given antibody among the total number of cells of each field, and counting at least ten fields. Specific normalization is indicated in the legend of each figure.

2.11 | Trichromic acid, Picro Sirius Red, and H&E histochemistry

Tissues were fixed in 4% of buffered formalin, embedded in paraffin blocks, sectioned at 5 μm and stained using the standard hematoxylin-eosin (Sigma-Aldrich) (H&E) method and Masson trichrome, briefly; samples were deparaffinized and rehydrate through 100% alcohol, 95% alcohol 70% alcohol, then, incubated in Bouin's solution at 60°C for 1 hour and

washed in running tap water for 5 minutes. Then stained in Weigert's working hematoxylin (Merck) for 1 minute, rinsed in running warm tap water for 10 minutes, and a last wash with distilled water. After were stained in Biebrich scarlet-acid fuchsin solution for 2 minutes, rinsed in distilled water, differentiated in phosphomolybdic-phosphotungstic acid solution for 15 minutes and 1% of acetic acid solution for 15 minutes and washed in distilled water. For Sirius red collagen staining, after deparaffinization and rehydration through 100% alcohol, 95% alcohol 70% alcohol, incubated with Picro-Sirius Red solution and after washing, subjected to two changes in acidified water. All preparations were dehydrated through 95% of ethyl alcohol, absolute ethyl alcohol, and clear in xylene. Samples were analyzed under a light microscopy by two pathologists blind to the treatment. All images were acquired using the Axiophot microscope (Zeiss), a direct microscope with transmitted light and epifluorescence (filters for DAPI, FITC and Red), using a DP70 (Olympus) color camera with the DP Controller image capture system. The objective used is a NEOFLUAR 40x objective. Image J was used to quantify the images, using color deconvolution to measure Picro-Sirius Red and Masson's Trichromic positive areas.

2.12 | Statistical analysis

For the statistical analysis of the results, the mean was taken as the measurement of the main tendency, while standard deviation (SD) was taken as the dispersion measurement. *T*-Student test was performed. The significance has been considered at $*P < .05$, ** for $P < .01$, and *** for $P < .001$. GraphPad Software v5.0 was used for statistical analysis and graphic representations.

3 | RESULTS

3.1 | GSE4 inhibits DNA damage, IL6 expression, and increases expression of TERC in bleomycin-treated RLE-6TN cells

Bleomycin has been used as a profibrotic drug in animal models of lung fibrosis that nicely reproduces many aspects of the disease found in IPF patients. Bleomycin (Bleo) induces pulmonary injury, inflammation, and subsequent fibrosis. In vitro Bleomycin induces DNA damage[38] and expression of pro-inflammatory cytokines in lung cells. Based on that, we analyze the role of GSE4 expression in recovering the cell damage caused by bleomycin, by transducing the rat lung epithelial cell line RLE-6TN, with lentiviral vectors expressing either scramble or GSE4 peptide (Figure S1A), and then, transduced cells were treated with different doses of bleomycin. First, telomerase activity was measured. Expression of GSE4 induced a significant increase of telomerase activity in bleomycin-treated cells (Figure 1A). Bleomycin did not affect telomerase activity, although higher doses of bleomycin reduced TERT gene expression (Figure 1B). RLE-6TN cells expressing GSE4 showed higher expression levels of TERT and TERC as compared to scramble vector, even after increasing doses of bleomycin (Figure 1B and C). In basal conditions, treatment of RLE-6TN cells with GSE-PLGA/PEI nanoparticles also induced expression of TERT (Figure S1B) as previously described for other disease cell lines.[28-30,39] Together these results suggest that the increase in telomerase activity obtained in GSE4/bleomycin-treated cells (Figure 1A) may be due to the increase in TERT and TERC gene expression in response to the damage induced by bleomycin.

RLE-6TN cells expressing scramble or GSE4 peptide when treated with increasing doses of bleomycin showed a dose-dependent increase of γ-H2A.X protein level that was inhibited by GSE4 expression (Figure 1D). Similar results were obtained treating RLE-6TN cells with PLGA/PEI nanoparticles loaded with scramble or GSE4 peptide (Figure S1C). We quantified the number of γ-H2A.X-associated foci per cell and found that GSE4 expression increased the number of cells with no-DNA damage at different bleomycin doses (Figure 1E and S1D). Further, we determined the number of telomere-associated foci (TIFs) and showed that GSE4 expression induced a small but statistically significant decrease of DNA damage at telomeres (Figure S2A and B) as described previously in other disease models.[28,30] Finally, we analyzed the DNA damage response by determining the activation of p53 by phosphorylation at serine[15]. We found an increase in p53 phosphorylation after bleomycin treatment that was attenuated in cells expressing GSE4 (Figure 2A). Accordingly, expression of CDKN1A also increased in a dose-dependent manner with bleomycin and this was also attenuated at the higher doses of bleomycin (Figure 2B). On the contrary, we did not detect differences in p16 expression in bleomycin-treated cells (not shown). When we analyzed the inflammatory response to bleomycin, we observed a reduction of IL-6 gene expression in GSE4 expressing cells compared to controls, were IL-6 was induced at any of the bleomycin doses tested (Figure 2C). This result was confirmed with GSE4-loaded nanoparticles, indicating that GSE4 was able, in vitro, to abolish the activation of bleomycin-induced expression of inflammation mediators (Figure S3).

Expression of pro-inflammatory cytokines is also involved in the activation of p38 MAPK.[30,40] We have found an increase in p38 phosphorylation in scramble cells with increasing concentrations of bleomycin that was not observed in GSE4-expressing cells (Figure 2D). Persistent activation of p38 MAPK is involved in apoptosis induction in response to DNA damaging agents.[41] Our data showed that the increased

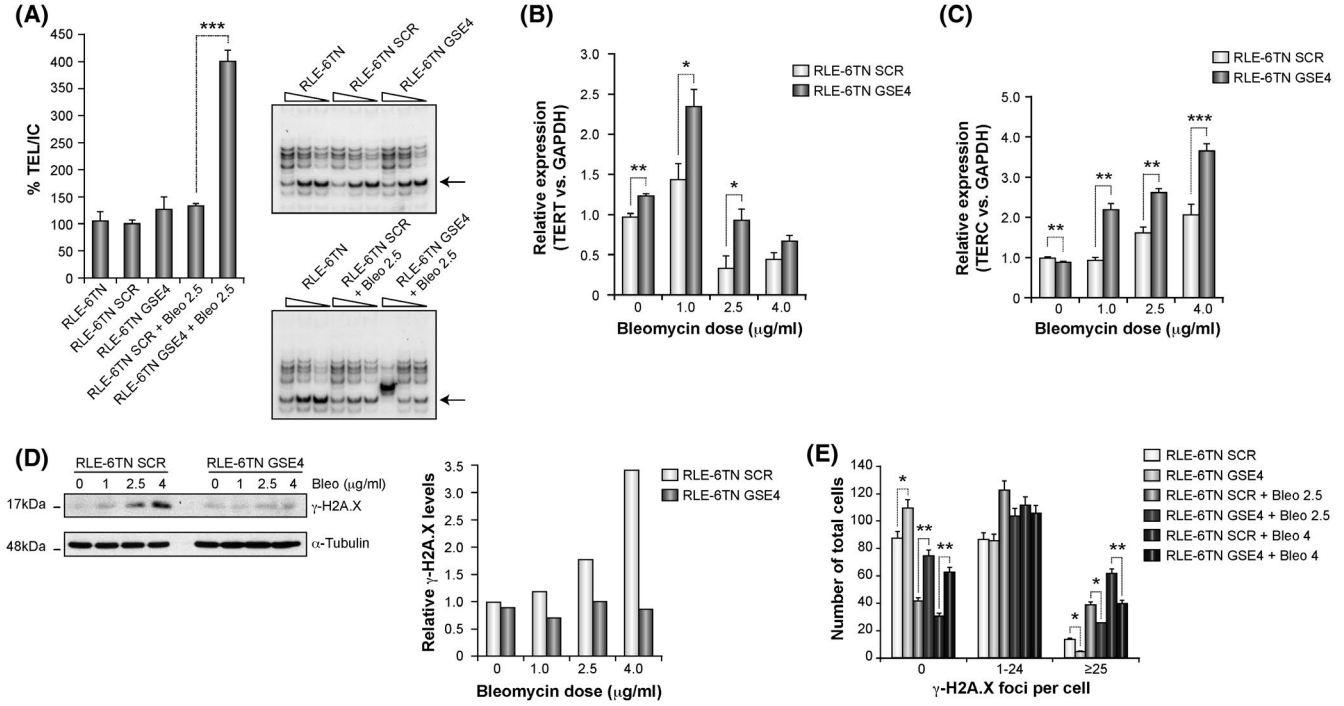

FIGURE 1 GSE4 expression increases telomerase activity and decreases DNA damage in bleomycin-treated RLE-6TN cells. A, Telomerase activity in RLE-6TN cells treated with bleomycin. RLE-6TN cells expressing scramble (SCR) or GSE4 peptides were treated with bleomycin (Bleo 2.5 μg/mL) for 6 hours when indicated. Telomerase activity was determined using the TRAP assay kit. Different extract dilutions were done for each sample (right panels). Telomerase activity was quantified and normalized by the internal control of amplification (arrow) of the kit and represented as relative activity (left panel). Data points represent the mean and standard deviations of two experiments performed in triplicate. The activity of non-transfected cells transfected was considered as 100% and all the others referred to that one. Asterisks indicated the statistical significance (* $P < .05$, ** $P < .01$, *** $P < .001$). B and C, Expression levels of TERT (B) and TERC (C) in RLE-6TN cells expressing either scramble (SCR) or GSE4 peptides and treated with bleomycin at the indicated concentrations for 6 hours. RNA was extracted and the expression of TERT and TERC measured by RT-q-PCR and data normalized with GADPH expression and referred to untreated RLE-6TN SCR cells. Asterisks indicated the statistical significance (* $P < .05$, ** $P < .01$, *** $P < .001$). D, RLE-6TN cells expressing scramble (SCR) or GSE4 peptides were treated with bleomycin at the indicated concentrations for 6 hours. Cells were lysed and the presence of γ-H2A.X and α-tubulin (loading control) analyzed by western blot (Left panel). Quantification values indicate the estimated ratio between γ-H2A.X and α-tubulin expression levels referred to those found in control RLE-6TN SCR cells. E, Quantification of γ-H2A.X-associated foci in RLE-6TN cells expressing either scramble (SCR) or GSE4. At least 200 cells were analyzed in each cell line and the number of foci/cell (among the total number of cells in the field) was divided into three groups. The number of cells in each group is indicated. Asterisks indicate significant differences between cell lines. Average values and standard deviations of two independent experiments are shown. Asterisks indicated the statistical significance (* $P < .05$, ** $P < .01$, *** $P < .001$)

ratio of cleaved-caspase 3/caspase 3 induced by bleomycin was reduced by GSE4 expression (Figure 2E) suggesting inhibition of apoptosis by this peptide.

3.2 | GSE4 inhibits the expression of TGF-β-induced genes in RLE-6TN cells

Since TGF-β is the most relevant profibrotic cytokine and with a relevant role in pulmonary fibrosis,[25,26] we studied the effect of TGF-β treatment in the expression of profibrotic genes in RLE-6TN cells. TGF-β treatment of RLE-6TN cells induces the expression of many genes related to the fibrotic phenotype (Figure 3) including α-smooth muscle actin (α-SMA), fibroblast growth factor (FGF-2), TGF-β receptor 1 (TGF-βR-1), vimentin, monocyte chemoattractant protein (MCP1), plasminogen activator inhibitor (PAI-1), TGF-β1, and collagen type I and III. GSE4 expression in rat AECs treated with TGF-β resulted in decreased expression levels of all these genes (Figure 3). We also observed that in the absence of TGF-β expression of GSE4 is also able to inhibit the expression of α-SMA, FGF2, and collagen type I and III as compared to control cells. Together these data indicated that GSE4 is able to inhibit the profibrotic response induced by TGF-β in rat AECs.

3.3 | In vivo treatment with GSE4-nanoparticles reduced lung damage and fibrosis

We used a rat model of intratracheal bleomycin-induced lung fibrosis in order to explore if treatment with

GSE4-nanoparticles was able on the first place to target lung cells and second to reduce lung damage and fibrosis in a more physiological model. Consequently, to test if GSE4 was able to target lung cells, we first performed a short treatment of rats by intraperitoneal inoculation of GSE4-nanoparticles 24 hours after the intratracheal bleomycin instillation. Three days later, we sacrificed the animals to test the effect of GSE4-nanoparticles treatment in the lungs. First, lung proteins were

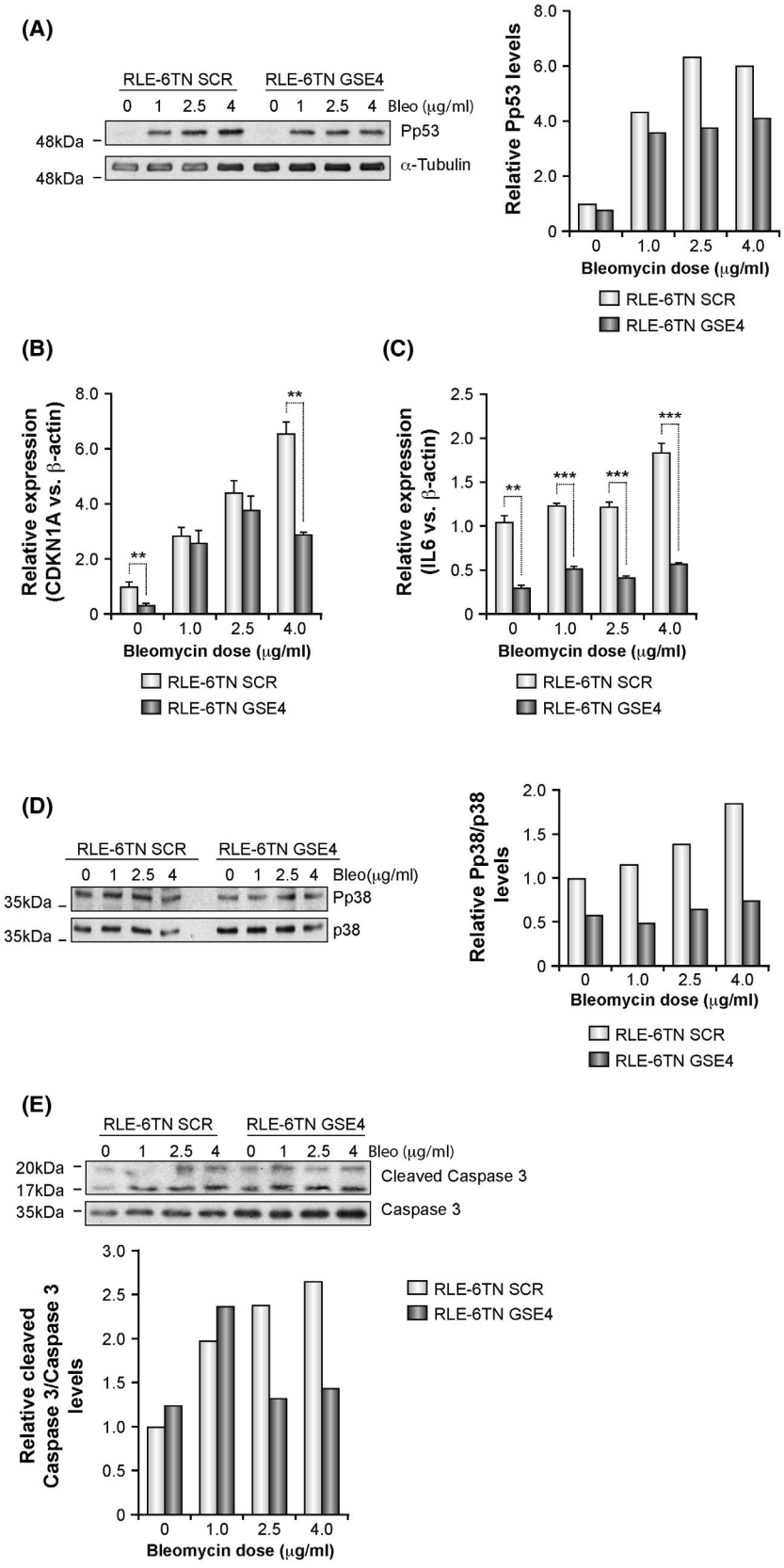

FIGURE 2 GSE4 decreases bleomycin-dependent expression of IL6, activated p38, and caspase 3 activity in RLE-6TN cells. A, Expression of Pp53 in RLE-6TN cells treated with bleomycin RLE-6TN cells expressing SCR or GSE4. Cells were lysed and the protein extracts used for western blot analysis of p53 phosphorylated at serine15 (Pp53) expression using a specific antibody and also with α-tubulin antibody as loading control (left panel). The ratio between the expression detected by both antibodies is indicated in the graphic at right, using RLE-6TN SCR cells as control. B, Expression of CDKN1A in RLE-6TN cells treated with bleomycin. RLE-6TN cells expressing scramble (SCR) or GSE4 peptides were treated with bleomycin at the indicated concentrations for 6 hours and total RNA extracted. The expression level of CDKN1A was estimated by RT-q-PCR with specific primers and β-actin expression used to normalize data. Expression was referred to untreated RLE-6TN SCR cells and represents data sets of three independent experiments. Asterisks indicated the statistical significance (* $P < .05$, ** $P < .01$, ***<0.001). C, Expression of IL-6 in RLE-6TN cells treated with bleomycin. RLE-6TN cells expressing scramble (SCR) or GSE4 peptides were treated with bleomycin at the indicated concentrations for 6 hours and total RNA extracted. The expression level of IL-6 was estimated by RT-q-PCR with specific primers and β-actin expression used to normalize data. Expression was referred to untreated RLE-6TN SCR cells and represents data sets of three independent experiments. Asterisks indicated the statistical significance (* $P < .05$, ** $P < .01$, ***<0.001). D, Expression of phosphorylated p38. RLE-6TN cells expressing SCR or GSE4 were lysed and the protein extracts used for western blot analysis of phospho-p38 expression using a specific antibody and also with a p38 antibody as loading control (upper panel). The ratio between the expression detected by both antibodies is indicated in the graphic bellow, using RLE-6TN SCR cells as control. The experiments were repeated three times with similar results. C) Caspase 3 activity. RLE-6TN cells expressing SCR or GSE4 were lysed and the protein extracts used for western blot analysis of caspase 3 expression, both the intact protein (caspase 3) and the products of activation (cleaved caspase 3) by using a specific antibody (upper panel). The ratio between expression detected by cleaved-caspase 3 and caspase 3 is indicated in the figure bellow using RLE-6TN SCR cells as control. A representative experiment is presented. The experiments were repeated three times with similar results

extracted from one lung and telomerase activity was measured. Our results showed that there was an increase (20%) in telomerase activity in rats treated with GSE4 compared with control lungs and this increased activity was sustained in lungs treated with bleomycin plus GSE4 (Figure 4A). In the other lung, we analyzed the expression of γ-H2AX in the pro-surfactant protein C positive (proSP-C) cells to determine if there was an inhibition of DNA damage by the expression in GSE4 in rat alveolar type II cells. We found that treatment with bleomycin increased the number of proSP-C positive cells expressing γ-H2A.X protein, and the number of positive cells decreased to levels similar to control cells when the rats were inoculated with GSE4-nanoparticles (Figure 4B), suggesting that GSE4 protects proSP-C cells from bleomycin treatment. In order to test if treatment with bleomycin was inducing fibrosis, we analyzed expression of the profibrotic marker α-SMA. The results indicated that there was an increase in the number of cells expressing α-SMA in the lungs of bleomycin-treated rats up to fourfold (Figure 4C) with respect to control lungs and this short GSE4 treatment slightly reduced it, indicating a decrease in myofibroblast-cell number. These results indicated that GSE4-nanoparticles were able to reach the lungs of the treated rats and reproduce an increase in telomerase activity observed on vitro even after bleomycin treatment and also to decrease DNA damage in proSP-C cells.

Using the same pulmonary fibrosis animal model, we studied the effect of GSE4-nanoparticles in two different protocols of treatment. In the preventive approach, rats were inoculated with GSE4-nanoparticles 1 day before the bleomycin treatment. For the therapeutic protocol, we inoculated GSE4-nanoparticles in rats 5 days after the bleomycin treatment when inflammatory/fibrotic process has already started. In both models, the injections of nanoparticles continued every 4 days until the end of the experiment (Figure 5A). We included three groups of rats for each protocol; untreated control, bleomycin, and bleomycin plus GSE4-nanoparticles inoculations. Rats were euthanized at day 14 since in our previous studies, we observed that fibrosis was already established at that time after bleomycin administration.[42]

Lung damage was determined in animals from both protocols by using CT scan (Figure 5B left panel) and histology at the end of the experiments. Figure 5C shows the quantitative representation of the CT images as density values (Hounsfield units (HU units)). For this quantification, we selected a volume of interest (VOI) that includes the whole lung. HU values correspond to the density of tissue, where values ranging from −1000 HU correspond to the air density and + 1000 HU to the bone density (Figure 5B, right panel). Quantitative analysis of the bleomycin group showed an increase in HUs by day 7 compared to controls (−300 to −175 for both protocols), corresponding to the inflammatory peak (Figure 5B and C) that persisted decreasing until day 14 (−275 to −75 preventive protocol and −300 to −125 therapeutic protocol) indicating the presence of fibrotic tissue. The administration of GSE4-nanoparticles was able to restrict the decrease of HU produced by bleomycin treatment in both experimental protocols (−300 to −220 preventive protocol and −300 to −250 therapeutic protocol at 14 days) (Figure 5B and C). At day 14, the control group exhibited no morphological alterations (Figure 5B), while the bleomycin group presented decreased lung volume due to the destruction of lung parenchyma and we observed the appearance of ground-glass opacities. CT image showed reduction of lung-damaged areas in the GSE4-nanoparticles-treated group (Figure 5B CT images). The tendency observed in the CT images was confirmed with SPECT acquisition by measuring ^{99m}Tc-MAA (microalbumin) distribution. We quantified ^{99m}Tc-MAA distribution images using

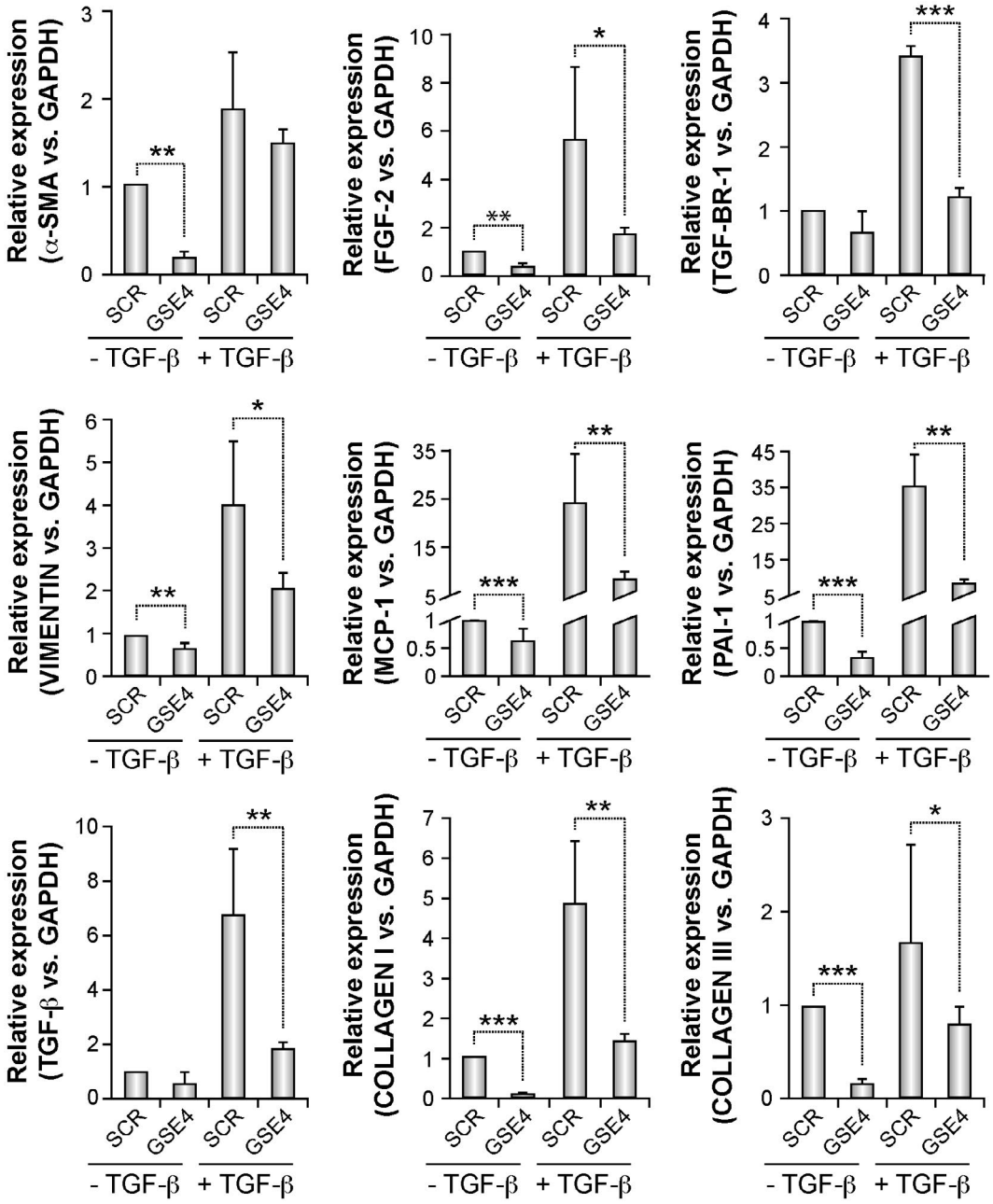

FIGURE 3 Expression of GSE4 inhibits the expression of TGF-β/fibrotic genes in RLE-6TN cells. RLE-6TN cells expressing scramble (SCR) or GSE4 peptides were treated when indicated with TGF-β (5 ng/mL) for 48 hours. Total RNA was extracted and the expression levels of the indicated genes estimated by RT-q-PCR with specific primers (Table 1). Data were normalized to GAPDH expression levels and are shown as mean ± SD of three independent experiments. Relative mRNA levels were normalized for those of scramble cell line (SCR) without TGF-β treatment. Asterisks indicated the statistical significance (* $P < .05$, ** $P < .01$, *** $P < .001$)

the therapeutic protocol (Figure 5E). The results showed an increase in the ^{99m}Tc uptake that in bleomycin group was diminishing as the disease progressed (day 0 to day 7), but the uptake in the bleomycin-GSE4-treated group was similar to bleomycin untreated controls, indicating that treatment with GSE4-nanoparticles normalized the intake of ^{99m}Tc, inhibited by bleomycin. In addition, we monitored the weight of the rats in both treatment protocols (Figure S4) and found that there is weight loss in rats treated with bleomycin at 14 days (8%) that is partially recovered when rats were treated with bleomycin + GSE4. Similar results were obtained for both preventive and therapeutic protocols.

Two-blinded independent pathologist examined the lung parenchymal lesions and accumulation of collagen in lung sections from different groups (Figure S5). Collagen was measured by both Mason´s Trichrome and Sirius red histological staining and that was quantified in the four experimental groups of rats. The control and GSE4-treated lungs showed

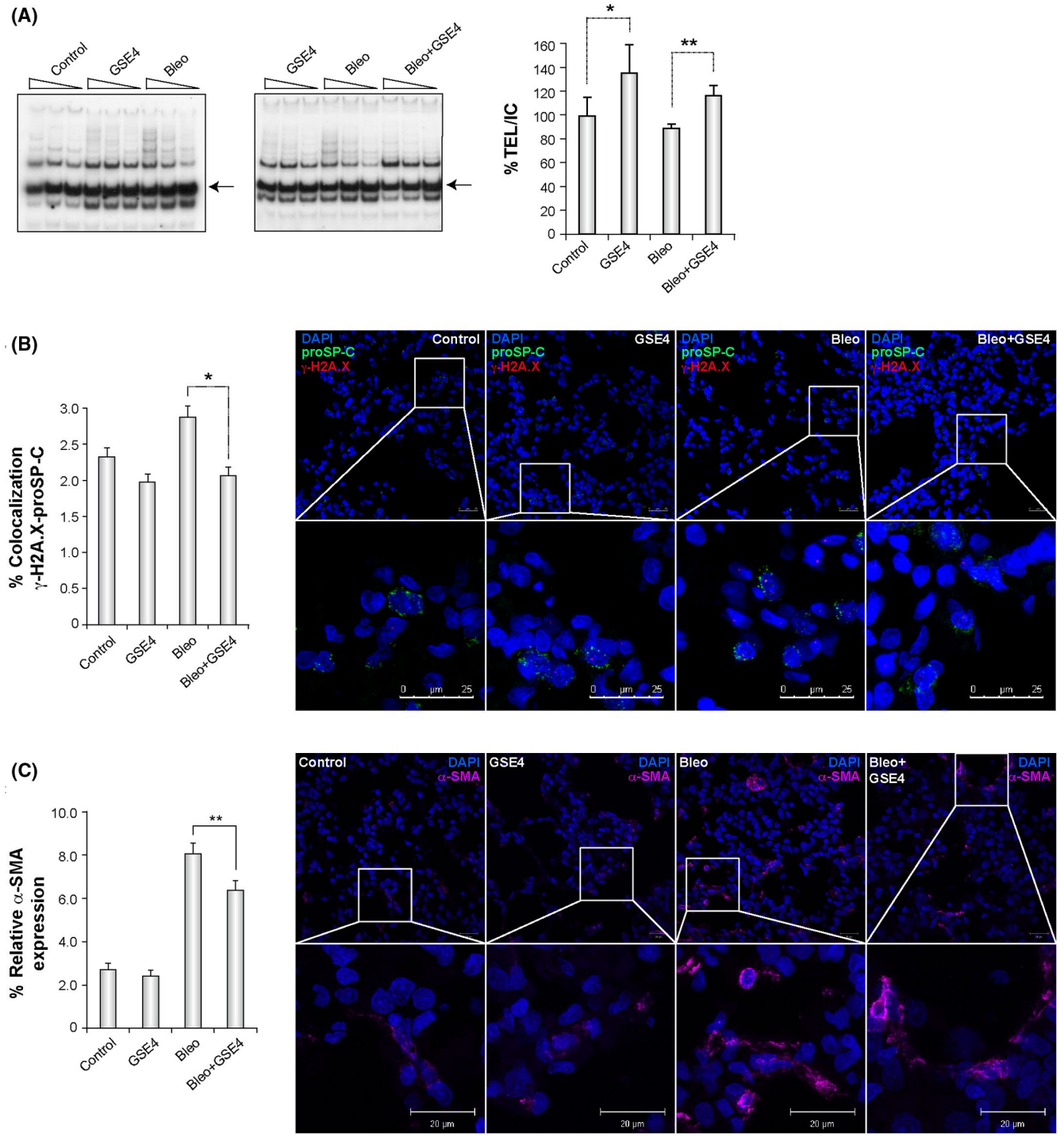

FIGURE 4 GSE4-nanoparticles recover telomerase activity and inhibit DNA damage at proSP-C cells in bleomycin-treated rats. A, Telomerase activity in lungs of GSE4-treated rats. Wistar rats were intratracheally instilled with a single dose of bleomycin (Bleo) 24 hours after being inoculated intraperitoneally once with GSE4-nanoparticles. Three days later one lung was used for TRAP assays. Twenty-four rats were used for each experiment and divided into four groups: control (n = 4), GSE4 (n = 4), Bleo (n = 8), and Bleo + GSE4 (n = 8). Different amounts of extracts were used for each TRAP assay (upper panel). Quantification of the intensity of the bands (TEL) in relation with the internal control (IC) (arrow) (TEL/IC) is presented (right panel). The experiments were repeated three times with similar results and average values and standard deviations of representative experiment showed (lower panel). Asterisks indicated the statistical significance (* $P < .05$, ** $P < .01$, *** $P < .001$). B, DNA damage in proSP-C + cells in GSE4-treated rats. One of the lungs isolated in A was used for immunohistochemistry detection of γ-H2A.X-associated foci and co-localization with proSP-C in each cell. The co-localization of both antigens was expressed as the percentage from total number of cells in 10 different fields for each analyzed lung. Right panel. C, Lungs from the experiment described in B) were subjected to immunohistochemistry to determine the expression of α-SMA (pink) and DAPI (blue). An insert for each picture showing amplified images is presented. The number of cells positive for α-SMA was determined in 10 different fields/rat and represented as the percentage of the total cell number per field. Asterisks indicated the statistical significance (* $P < .05$, ** $P < .01$, *** $P < .001$)

morphologically normal tissue with weak stain for collagen (Figure S5B and S5C). The bleomycin-treated group showed a clear interstitial alveolar involvement and collagen staining in fibrotic areas and parenchyma and increased expression of collagen. In contrast, the Bleo/GSE4-lungs showed that parenchymal architecture was better preserved, mild areas of

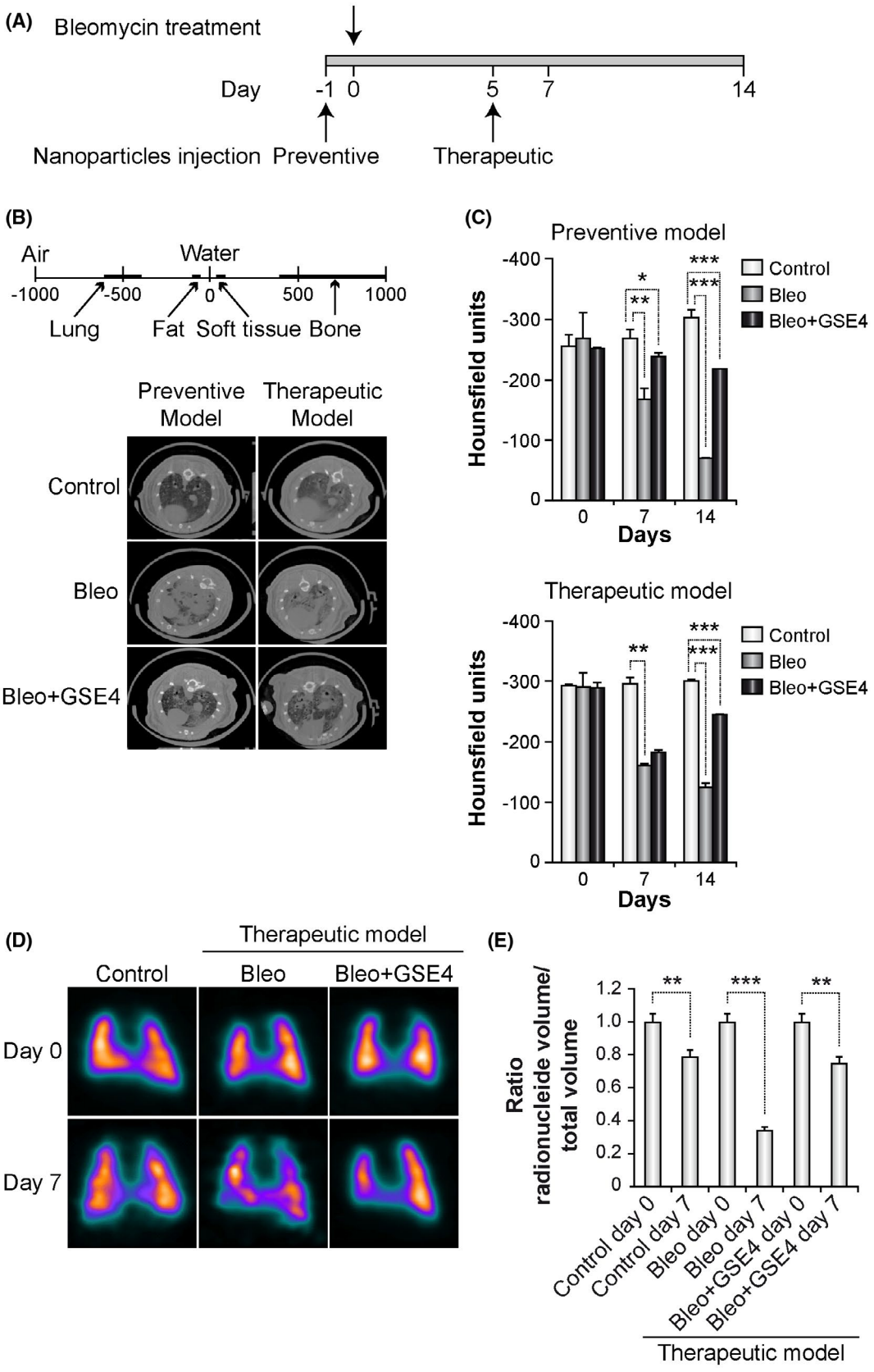

FIGURE 5 Bleomycin-induced fibrosis is attenuated by GSE4-loaded nanoparticles. A, Experimental design of preventive and therapeutic protocols. Bleomycin was intratracheally instilled at time 0 (upper arrow) while nanoparticles beginning at day −1 (preventive protocol) or 5 (therapeutic protocol) as indicated in the lower part of de diagram, later on, nanoparticles were inoculated intraperitoneally every 4 days. B, The Hounsfield scale (HS) and CT images. Upper panel HS of tissue density values: air as −1000 HU (minimum HU value), lung, fat, water (0 HU), soft tissue, and bone (+1000 HU). Lower panel representative SPECT acquisition images of rats subjected to CT scan of the lungs at day 14 after bleomycin instillation. Experimental groups correspond to rats: not treated (control, n = 4), bleomycin treated (Bleo, n = 8)) of bleomycin and GSE4 nanoparticles treated (Bleo + GSE4, n = 8)). C, Quantitative representation of CT technique in HS of the values of rat lungs of the preventive and therapeutic model from images taken at day 0, 7, and 14. Asterisks indicated the statistical significance (* $P < .05$, ** $P < .01$, *** $P < .001$). D, Images of ^{99m}Tc-MAA distribution in rats subjected to the therapeutic protocol. SPECT/CT acquisition images, on days 0 and 7; Images were analyzed and quantified by Analysis software PMOD 3.2. Experimental groups are Control, Bleomycin, and Bleo + GSE4. Representative images are presented. E, Quantification of images obtained in D (four rats/group), considering the radionuclide volume/total lung volume ratio. The data at experimental group at day 7 are referred to day 0. Asterisks indicated the statistical significance (* $P < .05$, ** $P < .01$, *** $P < .001$)

inflammatory infiltration were detected, and a statistically significant decrease in the collagen content was detected by both histological methods. These results indicated that the treatment with GSE4-nanoparticles in bleomycin-treated rats was able to protect from the massive cellular damage induced by bleomycin (Figure 5 and S5).

We also studied the expression levels of some pro-inflammatory cytokines such as IL6 and MCP1, whose expression was reduced by in vitro treatment or expression of GSE4 in RLE-6TN cells (Figures 2C, 3, and S3). We found that the expression levels of these two cytokines increased in lungs treated with bleomycin, and an important decrease in those rats treated with Bleo + GSE4 resembling the in vitro results (Figure S6A). Further, expression of TNF-α was also studied by immunohistochemistry and we found that treatment of rats with GSE4 already decreased a small basal expression of this cytokine (Figure S6B). Bleomycin induces an important increase and finally in Bleomycin + GSE4-treated rats, its expression is reduced by 50% (Figure S6B).

Next, we quantified the expression of proSP-C in order to investigate the damage and/or recovery of type II alveolar epithelial cells by GSE4 nanoparticles. We observed that bleo + GSE4-treated lungs showed an enrichment of 40% in multicellular alveoli-like structures (ranging from 2 to 5 cells per structure) expressing proSP-C when compared to the other treated groups (Figure 6A). This suggested that there was an increase in the number of proSP-C$^+$ cells induced by GSE4. To check if this correlated with an increase in cell proliferation of proSP-C cells, we tested the co-localization of Ki-67 and proSP-C in the lungs of the different groups. The results indicated that there was an increase in the number of Ki-67/proSP-C co-expressing cells when rats were treated with GSE4 alone, but interestingly increased more in Bleo + GSE4 rats (4,5%) (Figure 6B). We also studied the expression of the fibrotic marker α-SMA. The results indicated that there was an increase in the number of cells expressing α-SMA in the lungs of bleomycin-treated rats up to 10-fold (Figure 6C) and GSE4 treatment reduced to 5-fold indicating a decrease in myofibroblasts-cell number. Taken together, these results suggest that treatment with GSE4-nanoparticles after bleomycin resulted in an improvement of the lung repair capacity supported by the decrease in collagen content, fibrotic biomarkers, DNA damage, increased DNA synthesis, and a decrease in cytokine expression, and remarkably these results support also those obtained in the in vitro cell models.

4 | DISCUSSION

Idiopathic pulmonary fibrosis (IPF) occurs in genetically susceptible aged individuals exposed to several environmental risk factors.[8,12] In agreement with this observation in one-fourth of the cases this disease is associated with telomere shortening, which would impair lung stem cell function[17,20,43,44] and tissue repair.

Here, we describe that expression of GSE4 peptide in rat AECs reverts many of the pathological changes induced by bleomycin. Expression of GSE4 induced an important increase in telomerase activity. This activation on telomerase seems to be a consequence of increased expression of TERT and TERC genes in GSE4 expressing cells. We have also observed a decrease in DNA damage and DNA damage signaling in GSE4-RLE-6TN cells after bleomycin treatment. These results suggested that expression of GSE4 protects rat AECs from the bleomycin-induced damage. Similar results have been observed in response to DNA damage in other disease models such as dyskeratosis congenita (DC)[29,39] and ataxia telangiectasia (AT)[30] cells. More interestingly, DNA damage induced in telomeres by bleomycin is also slightly decreased by expression of GSE4, as already reported by expression of a similar peptide GSE24.2 in DC cells.[39]

Bleomycin also induced an increase in IL6 expression in RLE-6TN cells as already described for cells with persistent DNA damage.[30,45] Expression of GSE4 decreased IL6 expression in bleomycin-treated cells. Increased expression of this cytokine in AEC cells is involved in the inflammatory pathways that ultimately trigger a fibrotic process[46] and is also involved in the activation of p38 MAPK activity.[40] In

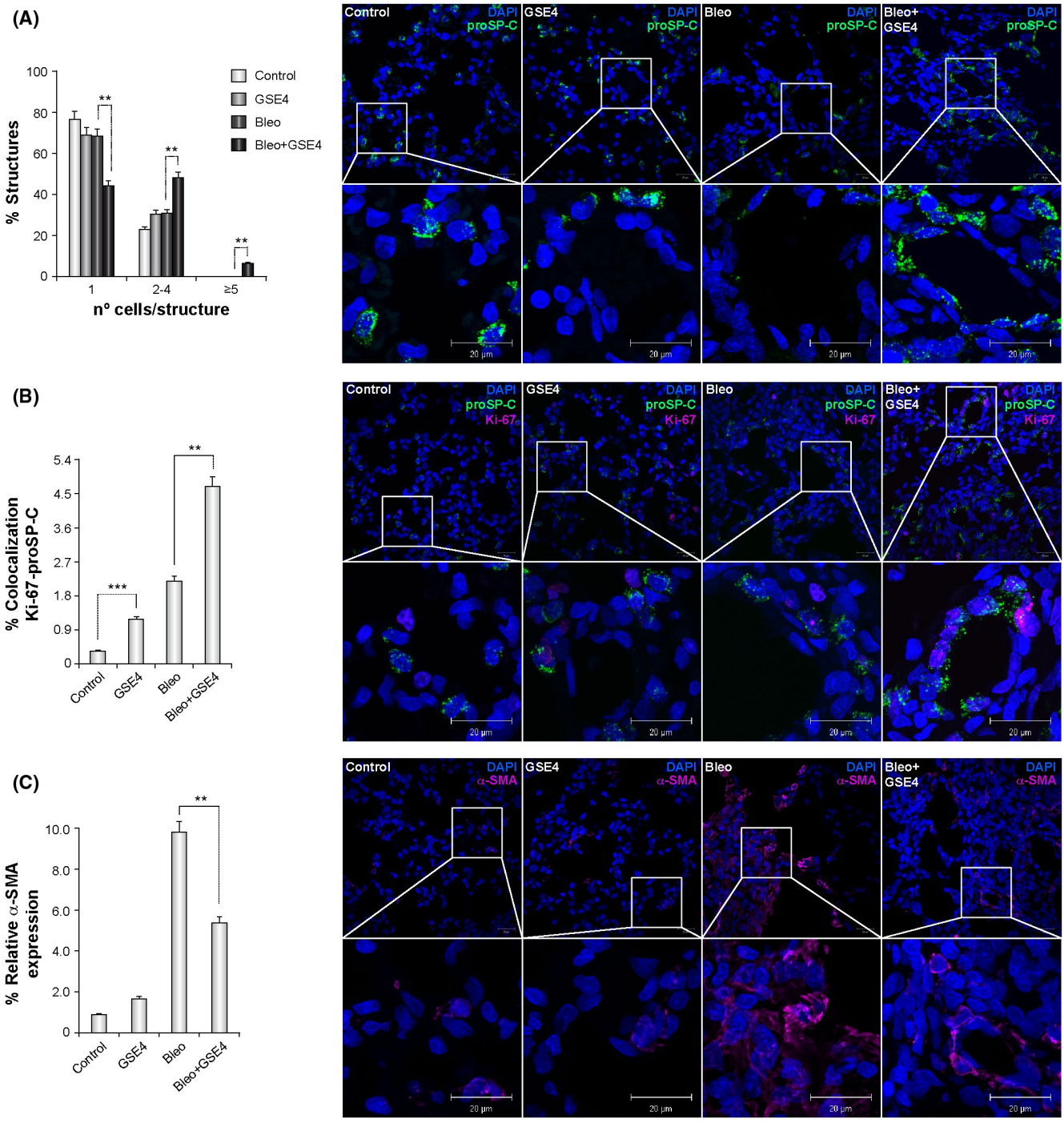

FIGURE 6 Treatment with GSE4-nanoparticles inhibits DNA damage in alveolar cells and decreases α-SMA expression. A, Right panel. Lungs from rats from each one of the therapeutic experimental groups: control (n = 4), GSE4 (n = 4), Bleo (n = 8), and Bleo + GSE4 (n = 8) were fixed and subjected to immunohistochemistry to determine the number of alveolar type II cells using proSP-C-specific antibody (green), nuclei were stained with DAPI (blue). An insert for each picture showing amplified images is presented. The number of pro-SPC$^+$ cells was determined in 10 different fields/rat and the number of pro-SPC$^+$ cells by alveolar structure determined. The data were grouped depending on the number of pro-SPC$^+$ cells per structure among the total structures in the field: 1, 2-4, and >5 as shown in left panel. B, Right Lungs from the experiment described in (A) were subjected to immunohistochemistry to determine the expression of Ki-67 (pink), proSP-C (green), and DAPI (blue). An insert for each picture showing amplified images is presented. The percentage of cells co-expressing Ki-67 and proSP-C (SPC) among the total cell number per field in 10 different fields/rat is represented in left panel. C, Right panel. Lungs from the experiment described in (A) were subjected to immunohistochemistry to determine the expression of α-SMA (pink) and DAPI (blue). An insert for each picture showing amplified images is presented. The number of cells positive for α-SMA was determined in 10 different fields/rat and represented as the percentage of the total cell number per field. For all panels, asterisks indicated the statistical significance (*$P < .05$, **$P < .01$, ***$P < .001$)

GSE4-RLE-6TN cells treated with bleomycin, the ratio of p38 activated/unphosphorylated p38 decreased in contrast to scramble-RLE-6TN cells. Bleomycin also increased apoptosis in RLE-6TN cells, in agreement with the described induction of apoptosis in pneumocytes of fibrotic animal models.[45] Expression of GSE4 in bleomycin-treated RLE-6TN cells decreases apoptosis. These results strongly indicated that GSE4 would counteract the cellular and DNA damage that is initiated by bleomycin in this cellular model.

One of the relevant cytokines in the fibrotic process in the lung is TGF-β, that contributes to change the expression of genes responsible for the epithelial to mesenchymal transition (EMT) that lead to fibrosis.[47] TGF-β-induced disturbances of the homeostatic microenvironment are critical to promote cell activation, migration, invasion, or hyperplastic changes.[47] In addition, excessive extracellular matrix production contributes in a major way to disease pathogenesis. Because of the relevance of TGF-β in lung fibrosis, the possible role of GSE4 on TGF-β-induced fibrosis in RLE-6TN cells was studied next. Interestingly, we found that expression of GSE4 in RLE-6TN cells decreased expression of genes involved in EMT. Moreover, GSE4 was also able to attenuate their induction in response to TGF-β, including those of COL1 and COL3 genes. These results agreed with others described for compounds with anti-fibrotic activity such as pirfenidone[48] or nintedanib.[49]

Type I and II pneumocytes are the major targets for lung damage in IPF. In a rat IPF model induced by bleomycin, inoculation of GSE4-nanoparticles rescued telomerase activity and decreased DNA damage in proSP-C cells confirming that GSE4-nanoparticles are active in these cells and would be suitable for in vivo treatment in a fibrosis model since they reach critical cells in the disease. We did not measure telomere length changes since the experiments were too short to produce them. Instead, we measure telomerase activity, describing an upregulation in GSE4-treated tissues that would be likely involved in protection from DNA damage induced by bleomycin. Increased DNA damage has been observed in explanted IPF lungs obtained from transplant surgeries compared to controls.[26] Further, increased p21 expression as a hallmark of aging and DNA damage has been reported in pulmonary fibrosis.[2] Our data demonstrates that treatment with GSE4 could prevent this feature.

Preventive and therapeutic protocols with GSE4-nanoparticles in rats treated with bleomycin showed promising results. In both situations, treatment with GSE4-nanoparticles was able to prevent and interfere with the lung damage induced by bleomycin as shown by the analyses of CT images obtained in the treated rats. Lung capacity also showed an improvement as assayed by the albumin ^{99m}Tc-MAA lung distribution. We also detected a decrease in expression pro-inflammatory cytokines such as IL6, MCP1, and TNF-α, besides collagen by GSE4. The expression of proSP-C in the lungs was used to determine alveolar structures containing more than two proSP-C cells. The results obtained suggested increased repair of alveolar structures induced by GSE4-nanoparticles. Additionally, this correlated with increased number of proliferative proSP-C cells. Finally, this treatment also inhibited the expression of the fibrotic marker α-SMA, further supporting that GSE4-nanoparticles protected proSP-C cells from the damage induced by bleomycin. PLGA nanoparticles have been used as an FDA approved delivery system for different drugs.[50] In addition, PLGA approved nanoparticles loaded with pirfenidone have previously been used in preclinical mice models of bleomycin-induced pulmonary fibrosis showing an anti-fibrotic activity.[51,52] This together with the evidence presented in this manuscript suggests that treatment with PLGA-GSE4-loaded nanoparticles would be a potential anti-fibrotic option for patients with lung fibrosis.

The only tested treatment for telomere diseases, like DC and IPF, is Danazol, which stimulates the estrogen-element at TERT promoter.[53,54] Although the results were promising, long-term treatments with this sexual hormone can have adverse side effects such as hepatic toxicity, lipid abnormalities, muscle problems, and of course the masculinization in women treated with this therapy, and as a consequence is not currently used.[54] In addition, it has been suggested that extrapulmonary alterations in other cell types, like the bone marrow mesenchymal stem cells (B-MSCs) from IPF patients, that have a premature senescence phenotype, might contribute to the pathogenesis of the disease. Moreover, it was demonstrated that infusion of B-MSCs isolated from normal young donors in the initial stages of the injury results in a decrease in collagen deposition in the lungs after bleomycin instillation and milder fibrosis.[55] Since GSE4 is able to increase telomerase activity, decrease DNA damage and induce survival in lymphoblasts derived from DC patients,[29] it is tempting to suggest that GSE4 could improve the beneficial activity of B-MSCs. In the same line, it would be interesting to investigate the use of GSE4 in lung fibrosis patients with short telomeres, since besides helping to recover lung damage would also contribute to overcome the blood abnormalities found in these patients without the side effects of the anti-fibrotic therapies.[56]

There are limitations in our current study. We have used a lung fibrosis model, using bleomycin as a fibrotic inducer that does not recapitulate some features of IPF pathology such as mortality. This could be due to the partial reversibility of the injure at later timepoints and to the lack in alterations in other cells types (B-MSC), so it may not represent the complexity of the disease. Still, approved treatments for IPFs such as pirfenidone and nintedanib, were tested in this model since is the only existing one. On the contrary, we need to develop genetic mice models to induce GSE4 in specific cell types, such as alveolar type II cells and compare it to the

expression in lung fibroblasts to define its cell type-specific functions. Further, it would be interesting to assay if treatment with GSE4-nanoparticles would have impact on IPF induced in a short telomere mice model.

Altogether, the results presented here demonstrate that treatment of lung damage induced by bleomycin with GSE4-nanoparticles, decreases DNA damage, activates telomerase activity, decreases inflammation, apoptosis, and EMT, resulting in a decreased lung fibrosis, and increased number of alveolar cells. No deleterious, but beneficial effects have been observed by GSE4 treatment in different disease-derived cell models (DC, AT), in contrast to the toxicity observed in the actual IPF treatments that in addition have limited beneficial effects. Therefore, the use of GSE4-nanoparticles should be considered and more deeply explored as an alternative treatment for lung fibrotic patients.

ACKNOWLEDGMENTS

R.P laboratory was funded by grants P17-01401 (Fondo de Investigaciones Sanitarias, Instituto de Salud Carlos III, Spain supported by FEDER funds), CIBER 576/805_ER16PE06P2016 and MINECO from the Spanish Government (INNPACTO, IPT-2012-0674-090000). M.M-M. laboratory was funded by Instituto de Salud Carlos III PI18/00367, supported by FEDER (Fondos Europeos de Desarrollo Regional (a way to build Europe)), JC received funds from MINECO CICYT SAF2014-55322-P, and GG laboratory was funded by grant SAF2015-68073-R (MINECO/FEDER) supported by FEDER funds. C.MG and R G-L are granted by the CIBERER. We gratefully acknowledge to CNB IIB histology Monica Martin Belinchón for technical assistance in the microscopy core facility and Ana Sastre-Perona for helpful comments about the manuscript.

AUTHOR CONTRIBUTIONS

RP, LS, and MM-M conceived and designed research and wrote the paper. JC and AS performed research rat in vivo studies and processed all the image data. LP-B, AM-W, BF-V, R G-L, and LP-B performed most in vitro work. GG contributed with the vectors used in the cell assays. CM-G and EG-AS performed research processed the in vivo samples for immunohistochemistry. LI, SPE, RMH, MI, and JLP, performed research obtained and characterized the PLGA/PEI nanoparticles. All authors critically revised the manuscript for important intellectual content.

ORCID

Rosario Perona https://orcid.org/0000-0002-2973-5153

REFERENCES

1. Raghu G, Collard HR, Egan JJ, et al. An official ATS/ERS/JRS/ALAT statement: idiopathic pulmonary fibrosis: evidence-based guidelines for diagnosis and management. *Am J Respir Crit Care Med*. 2011;183:788-824.
2. Selman M, Pardo A. Revealing the pathogenic and aging-related mechanisms of the enigmatic idiopathic pulmonary fibrosis. an integral model. *Am J Respir Crit Care Med*. 2014;189:1161-1172.
3. Raghu G, Anstrom KJ, King TE Jr, Lasky JA, Martinez FJ. Prednisone, azathioprine, and N-acetylcysteine for pulmonary fibrosis. *N Engl J Med*. 2012;366:1968-1977.
4. Ng B, Dong J, D'Agostino G, et al. Interleukin-11 is a therapeutic target in idiopathic pulmonary fibrosis. *Sci Transl Med*. 2019;11(511):eaaw1237. https://doi.org/10.1126/scitranslmed.aaw1237
5. Richeldi L, du Bois RM, Raghu G, et al. Efficacy and safety of nintedanib in idiopathic pulmonary fibrosis. *N Engl J Med*. 2014;370:2071-2082.
6. King TE Jr, Bradford WZ, Castro-Bernardini S, et al. A phase 3 trial of pirfenidone in patients with idiopathic pulmonary fibrosis. *N Engl J Med*. 2014;370:2083-2092.
7. Mora AL, Rojas M, Pardo A, Selman M. Emerging therapies for idiopathic pulmonary fibrosis, a progressive age-related disease. *Nat Rev Drug Discov*. 2017;16:810.
8. Armanios M, Blackburn EH. The telomere syndromes. *Nat Rev Genet*. 2012;13:693-704.
9. Konigshoff M. Lung cancer in pulmonary fibrosis: tales of epithelial cell plasticity. *Respiration*. 2011;81:353-358.
10. Povedano JM, Martinez P, Serrano R, et al. Therapeutic effects of telomerase in mice with pulmonary fibrosis induced by damage to the lungs and short telomeres. *Elife*. 2018;7:e31299.
11. Naikawadi RP, Disayabutr S, Mallavia B, et al. Telomere dysfunction in alveolar epithelial cells causes lung remodeling and fibrosis. *JCI Insight*. 2016;1:e86704.
12. Perona R, Iarriccio L, Pintado-Berninches L, et al. Molecular diagnosis and precision therapeutic approaches for telomere biology disorders. In: M. L. Larramendy (Ed.), *Telomere—A complex end of a chromosome*. Intech; 2016:77-117.
13. Stanley SE, Gable DL, Wagner CL, et al. Loss-of-function mutations in the RNA biogenesis factor NAF1 predispose to pulmonary fibrosis-emphysema. *Sci Transl Med*. 2016;8:351ra107.
14. Hoffman TW, van der Vis JJ, van der Smagt JJ, Massink MPG, Grutters JC, van Moorsel CHM. Pulmonary fibrosis linked to variants in the ACD gene, encoding the telomere protein TPP1. *Eur Respir J*. 2019;54(6):1900809.
15. Kannengiesser C, Manali ED, Revy P, et al. First heterozygous NOP10 mutation in familial pulmonary fibrosis. *Eur Respir J*. 2020;55(6):1902465.
16. Benyelles M, O'Donohue MF, Kermasson L, et al. NHP2 deficiency impairs rRNA biogenesis and causes pulmonary fibrosis and H$\sqrt{\prod}$yeraal-Hreidarsson syndrome. *Hum Mol Genet*. 2020;29:907-922.
17. Hoffman TW, van Moorsel CHM, Borie R, Crestani B. Pulmonary phenotypes associated with genetic variation in telomere-related genes. *Curr Opin Pulm Med*. 2018;24:269-280.
18. Liu YY, Shi Y, Liu Y, Pan XH, Zhang KX. Telomere shortening activates TGF-beta/Smads signaling in lungs and enhances both lipopolysaccharide and bleomycin-induced pulmonary fibrosis. *Acta Pharmacol Sin*. 2018;39:1735-1745.
19. Stanley SE, Chen JJ, Podlevsky JD, et al. Telomerase mutations in smokers with severe emphysema. *J Clin Invest*. 2015;125:563-570.

20. Chen R, Zhang K, Chen H, et al. Telomerase deficiency causes alveolar stem cell senescence-associated low-grade inflammation in lungs. *J Biol Chem*. 2015;290:30813-30829.
21. Willis BC, Borok Z. TGF-beta-induced EMT: mechanisms and implications for fibrotic lung disease. *Am J Physiol Lung Cell Mol Physiol*. 2007;293:L525-534.
22. Willis BC, duBois RM, Borok Z. Epithelial origin of myofibroblasts during fibrosis in the lung. *Proc Am Thorac Soc*. 2006;3:377-382.
23. Willis BC, Liebler JM, Luby-Phelps K, et al. Induction of epithelial-mesenchymal transition in alveolar epithelial cells by transforming growth factor-beta1: potential role in idiopathic pulmonary fibrosis. *Am J Pathol*. 2005;166:1321-1332.
24. Antoniades HN, Bravo MA, Avila RE, et al. Platelet-derived growth factor in idiopathic pulmonary fibrosis. *J Clin Invest*. 1990;86:1055-1064.
25. Khalil N, O'Connor RN, Flanders KC, Unruh H. TGF-beta 1, but not TGF-beta 2 or TGF-beta 3, is differentially present in epithelial cells of advanced pulmonary fibrosis: an immunohistochemical study. *Am J Respir Cell Mol Biol*. 1996;14:131-138.
26. Goldmann T, Zissel G, Watz H, et al. Human alveolar epithelial cells type II are capable of TGFbeta-dependent epithelial-mesenchymal-transition and collagen-synthesis. *Respir Res*. 2018;19(1):138.
27. Machado-Pinilla R, Sanchez-Perez I, Murguia JR, Sastre L, Perona R. A dyskerin motif reactivates telomerase activity in X-linked dyskeratosis congenita and in telomerase-deficient human cells. *Blood*. 2008;111:2606-2614.
28. Manguan-Garcia C, Pintado-Berninches L, Carrillo J, et al. Expression of the genetic suppressor element 24.2 (GSE24.2) decreases DNA damage and oxidative stress in X-linked dyskeratosis congenita cells. *PLoS One*. 2014;9:e101424.
29. Iarriccio L, Manguan-Garcia C, Pintado-Berninches L, et al. GSE4, a small dyskerin- and GSE24.2-related peptide, induces telomerase activity, cell proliferation and reduces DNA damage, oxidative stress and cell senescence in dyskerin mutant cells. *PLoS One*. 2015;10:e0142980.
30. Pintado-Berninches L, Fernandez-Varas B, Benitez-Buelga C, et al. GSE4 peptide suppresses oxidative and telomere deficiencies in ataxia telangiectasia patient cells. *Cell Death Differ*. 2019;26(10):1998-2014.
31. Egusquiaguirre SP, Manguan-Garcia C, Pintado-Berninches L, et al. Development of surface modified biodegradable polymeric nanoparticles to deliver GSE24.2 peptide to cells: a promising approach for the treatment of defective telomerase disorders. *Eur J Pharm Biopharm*. 2015;91:91-102.
32. Egusquiaguirre SP, Manguan-Garcia C, Perona R, Pedraz JL, Hernandez RM, Igartua M. Development and validation of a rapid HPLC method for the quantification of GSE4 peptide in biodegradable PEI-PLGA nanoparticles. *J Chromatogr B Analyt Technol Biomed Life Sci*. 2014;972:95-101.
33. Almudever P, Milara J, De Diego A, et al. Role of tetrahydrobiopterin in pulmonary vascular remodelling associated with pulmonary fibrosis. *Thorax*. 2013;68:938-948.
34. Cortijo J, Iranzo A, Milara X, et al. Roflumilast, a phosphodiesterase 4 inhibitor, alleviates bleomycin-induced lung injury. *Br J Pharmacol*. 2009;156:534-544.
35. Milara J, Morcillo E, Monleon D, Tenor H, Cortijo J. Roflumilast prevents the metabolic effects of bleomycin-induced fibrosis in a murine model. *PLoS One*. 2015;10:e0133453.
36. Giulietti A, Overbergh L, Valckx D, Decallonne B, Bouillon R, Mathieu C. An overview of real-time quantitative PCR: applications to quantify cytokine gene expression. *Methods*. 2001;25:386-401.
37. Sasser TA, Chapman SE, Li S, et al. Segmentation and measurement of fat volumes in murine obesity models using X-ray computed tomography. *J Vis Exp*. 2012;e3680.
38. Mouratis MA, Aidinis V. Modeling pulmonary fibrosis with bleomycin. *Curr Opin Pulm Med*. 2011;17:355-361.
39. Machado-Pinilla R, Carrillo J, Manguan-Garcia C, et al. Defects in mTR stability and telomerase activity produced by the Dkc1 A353V mutation in dyskeratosis congenita are rescued by a peptide from the dyskerin TruB domain. *Clin Transl Oncol*. 2012;14:755-763.
40. Freshney NW, Rawlinson L, Guesdon F, et al. Interleukin-1 activates a novel protein kinase cascade that results in the phosphorylation of Hsp27. *Cell*. 1994;78:1039-1049.
41. Jang S, Ryu SM, Lee J, et al. Bleomycin inhibits proliferation via schlafen-mediated cell cycle arrest in mouse alveolar epithelial cells. *Tuberc Respir Dis (Seoul)*. 2019;82:133-142.
42. Milara J, Hernandez G, Ballester B, et al. The JAK2 pathway is activated in idiopathic pulmonary fibrosis. *Respir Res*. 2018;19(1):24.
43. Armanios M. Telomerase and idiopathic pulmonary fibrosis. *Mutat Res*. 2012;730:52-58.
44. Alder JK, Barkauskas CE, Limjunyawong N, et al. Telomere dysfunction causes alveolar stem cell failure. *Proc Natl Acad Sci USA*. 2015;112:5099-5104.
45. Duffield JS, Lupher M, Thannickal VJ, Wynn TA. Host responses in tissue repair and fibrosis. *Annu Rev Pathol*. 2013;8:241-276.
46. Liu Y, Lu F, Kang L, Wang Z, Wang Y. Pirfenidone attenuates bleomycin-induced pulmonary fibrosis in mice by regulating Nrf2/Bach1 equilibrium. *BMC Pulm Med*. 2017;17:63.
47. Fernandez IE, Eickelberg O. The impact of TGF-beta on lung fibrosis: from targeting to biomarkers. *Proc Am Thorac Soc*. 2012;9:111-116.
48. Inomata M, Kamio K, Azuma A, et al. Pirfenidone inhibits fibrocyte accumulation in the lungs in bleomycin-induced murine pulmonary fibrosis. *Respir Res*. 2014;15(1):16.
49. Li LF, Kao KC, Liu YY, et al. Nintedanib reduces ventilation-augmented bleomycin-induced epithelial-mesenchymal transition and lung fibrosis through suppression of the Src pathway. *J Cell Mol Med*. 2017;21:2937-2949.
50. Ding D, Zhu Q. Recent advances of PLGA micro/nanoparticles for the delivery of biomacromolecular therapeutics. *Mater Sci Eng C Mater Biol Appl*. 2018;92:1041-1060.
51. Chowdhury S, Guha R, Trivedi R, Kompella UB, Konar A, Hazra S. Pirfenidone nanoparticles improve corneal wound healing and prevent scarring following alkali burn. *PLoS One*. 2013;8:e70528.
52. Trivedi R, Redente EF, Thakur A, Riches DW, Kompella UB. Local delivery of biodegradable pirfenidone nanoparticles ameliorates bleomycin-induced pulmonary fibrosis in mice. *Nanotechnology*. 2012;23:505101.
53. Townsley DM, Dumitriu B, Liu D, et al. Danazol treatment for telomere diseases. *N Engl J Med*. 2016;374:1922-1931.
54. Calado RT, Yewdell WT, Wilkerson KL, et al. Sex hormones, acting on the TERT gene, increase telomerase activity in human primary hematopoietic cells. *Blood*. 2009;114:2236-2243.

55. Cardenes N, Alvarez D, Sellares J, et al. Senescence of bone marrow-derived mesenchymal stem cells from patients with idiopathic pulmonary fibrosis. *Stem Cell Res Ther*. 2018;9:257.
56. Planas-Cerezales L, Arias-Salgado EG, Buendia-Roldan I, et al. Predictive factors and prognostic effect of telomere shortening in pulmonary fibrosis. *Respirology*. 2019;24:146-153.

SUPPORTING INFORMATION

Additional supporting information may be found online in the Supporting Information section.

How to cite this article: Pintado-Berninches L, Montes-Worboys A, Manguan-García C, et al. GSE4-loaded nanoparticles a potential therapy for lung fibrosis that enhances pneumocyte growth, reduces apoptosis and DNA damage. *The FASEB Journal*. 2021;35:e21422. https://doi.org/10.1096/fj.202001160RR